THE JOURNAL OF BIOLOGICAL CHEMISTRY
Vol. 279, No. 14, Issue of April 2, pp. 13425–13434, 2004

Printed in U.S.A.

Stopped-flow Fluorescence Studies of Inhibitor Binding to Tyrosinase from *Streptomyces antibioticus**

Received for publication, August 25, 2003, and in revised form, December 19, 2003
Published, JBC Papers in Press, December 29, 2003, DOI 10.1074/jbc.M309367200

Armand W. J. W. Tepper‡, Luigi Bubacco§, and Gerard W. Canters‡¶

From the ‡Leiden Institute of Chemistry, Gorlaeus Laboratories, Leiden University, Einsteinweg 55, 2333 CC, Leiden, The Netherlands and the §Department of Biology, University of Padua, Via Trieste 75, 30121 Padua, Italy

Tyrosinase (Ty) is a type 3 copper protein involved in the rate-limiting step of melanin synthesis. It is shown that the endogenous Trp fluorescence of tyrosinase from *Streptomyces antibioticus* is remarkably sensitive to the redox state. The fluorescence emission intensity of the [(Cu(I) Cu(I)] reduced species is more than twice that of the oxygen-bound [Cu(II)-O_2^{2-}-Cu(II)] form. The emission intensity of the oxidized [Cu(II)-OH^--Cu(II)] protein (Ty_{met}) appears to be dependent on an acid-base equilibrium with a pK_a value of 4.5 ± 0.1. The binding of fluoride was studied under pseudo first-order conditions using stopped-flow fluorescence spectroscopy. The kinetic parameters k_{on}, K_d, and the fraction of fluorescence emission quenched upon fluoride binding show a similar pH dependence as above with an average pK_a value of 4.62 ± 0.05. Both observations are related to the dissociation of Cu_2-bridging hydroxide at low pH. It is further shown that Ty is rapidly inactivated at low pH and that halide protects the enzyme from this inactivation. All results support the hypothesis that halide displaces hydroxide as the Cu_2-bridging ligand in Ty_{met}. The relevance of the experimental findings for the catalytic cycle is discussed. The data are consistent with the data obtained from other techniques, validating the use of fluorescence quenching as a sensitive and effective tool in studying ligand binding and substrate conversion.

The details of the interaction of inhibitors with the dinuclear copper enzyme tyrosinase (Ty[1]; EC 1.14.18.1) are still far from being completely understood. They are the subject of this report. Tyrosinases are involved in the rate-limiting step in the synthesis of melanin pigments, which fulfill various roles in living organisms. In mammals, melanins are responsible for skin, eye, inner ear, and hair pigmentation, and defects in Ty are related to a range of medical conditions like type I human oculocutaneous albinism (1, 2). In fruits and mushrooms, melanin formation is responsible for the browning of tissue occurring after bruising or long storage time (3), and in insects it is thought that melanins assist in wound healing and sclerotization of the cuticle (4).

In eukaryotes, the melanogenic pathway is complex and involves several enzymatic and non-enzymatic steps (5). The pathway starts with the Ty-catalyzed hydroxylation and subsequent oxidation of L-tyrosine to L-DOPAquinone, which is then converted to DOPAchrome. DOPAchrome, in turn, is a precursor in the synthesis of polyphenolic melanin pigments. Although the Ty activity has been studied for over a century (see Refs. 3–7 for recent reviews), both the enzyme structure and its detailed mechanism of action remain to be solved.

Tyrosinase contains a so-called type 3 copper site that is composed of two closely spaced copper ions, which are each coordinated by 3 histidine residues (4, 8). The type 3 site also occurs in the hemocyanins (Hcs), which function as oxygen carriers and storage proteins in arthropods and molluscs, and in the plant catechol oxidases (COs), which oxidize diphenols to the corresponding quinones but lack the Ty hydroxylation activity. Although the type 3 proteins fulfill different functions, the dinuclear active site seems to be highly conserved as witnessed by its characteristic spectroscopic signatures and the available crystal structures for several Hcs (9–11) and a catechol oxidase (12). The differences in functionality are therefore thought to derive from variations in the accessibility of substrates to the active site or the ability of substrates to appropriately dock into the active center (7, 13, 14).

The Ty type 3 site can exist in various forms as follows: (*a*) the [Cu(I) Cu(I)]-reduced Ty_{red} species; and (*b*) the [Cu(II)-O_2^{2-}-Cu(II)] Ty_{oxy} species, in which molecular oxygen is bound as peroxide in a μ-η^2:η^2 side bridging mode to the Cu_2 center. The Ty_{oxy} form, which results from the binding of molecular oxygen to Ty_{red}, is competent to react with both monophenols and diphenols and is characterized by a strong ligand to metal charge transfer (LMCT) band centered around 345 nm and a low O-O stretching vibration frequency of ~750 cm^{-1} (4). (*c*) The [Cu(II)-OH^--Cu(II)]-oxidized met form (Ty_{met}) is competent to react with diphenols only. The Ty_{met} form results when Ty_{oxy} reacts with a diphenol to produce the corresponding quinone.

Detailed knowledge of the interaction of Ty with its inhibitors is of paramount importance for understanding the Ty enzyme mechanism, as well as for the development of novel Ty inhibitors relevant to skin treatment and the economically important prevention of the browning of fruits, vegetables, and mushrooms, for example. Consequently, steady-state kinetic studies of Ty inhibition are abundant, and many inhibitors have been identified (*e.g.* Refs. 15–24). Yet direct spectroscopic investigations of inhibitor binding to tyrosinases have been few, partly because of the scarcity of suitable spectroscopic probes. For example, Ty_{met} shows no strong UV-visible absorption bands and is EPR-silent due to the antiferromagnetic coupling between the two unpaired spins on the copper ions (4). Spectroscopic studies mainly pertained to the half-oxidized

* The costs of publication of this article were defrayed in part by the payment of page charges. This article must therefore be hereby marked "*advertisement*" in accordance with 18 U.S.C. Section 1734 solely to indicate this fact.

¶ To whom correspondence should be addressed: Leiden University, Einsteinweg 55, P. O. Box 9502, 2300 RA Leiden, The Netherlands. Tel.: 31-71-527-4256; Fax: 31-71-527-4349; E-mail: canters@chem.leidenuniv.nl.

[1] The abbreviations used are: Ty, tyrosinase; Hcs, hemocyanins; LMCT, ligand to metal charge transfer; L-DOPA, 3,4-dihydroxy-L-phenylalanine; COs, catechol oxidases.

species, in which one of the copper ions in the active site occurs in the Cu(II) and the other in the Cu(I) oxidation state ($Ty_{half\text{-}met}$), rendering the site suitable for study by EPR techniques. Although EPR studies on $Ty_{half\text{-}met}$ have yielded much information regarding the coordination geometry of the oxidized copper and the changes that occur when ligands bind to the active site, the half-met form does not occur naturally and the technique allows for the investigation of only one of the copper ions in the type 3 site.

It was a step forward recently when the oxidized Ty_{met} derivative appeared amenable to paramagnetic NMR (8, 25, 26); the $S = 1$ spin state of Ty_{met} was found to be thermally accessible at room temperature, providing sufficient paramagnetism for the signals of the coordinating histidine protons to shift outside the diamagnetic envelope. The NMR studies demonstrated that also Ty contains a classical type 3 site in which, like in Hcs and COs, the two copper ions are coordinated by six histidine residues through their Nϵ atoms (8). Furthermore, large changes in the Ty_{met} paramagnetic ^1H NMR spectrum are observed when inhibitors bind to the active site (25, 26), allowing us to follow ligand binding and to obtain structural information on the complexes. For instance, it was shown that halides interact with both the oxidized and reduced Ty, where the affinity for halide ion and the mechanism of inhibition depend both on the nature of the halide ion and the oxidation state of the type 3 site (26) (K_d^{red}, $I^- < Br^- < Cl^- \ll F^-$; K_d^{met}, $F^- < Cl^- < Br^- \ll I^-$). The binding of halide to Ty_{met} is strongly pH-dependent, *i.e.* halide only binds to the acidic form of the enzyme, resulting in stronger inhibition with decreasing pH. As a consequence of the instability of the enzyme at low pH and of the relatively long experimental times required, in the past we were able to estimate only an upper limit of 5.5 for the pK_a of the process modulating the halide binding (26). In the same study it was also proposed that halides bridge the two copper ions in the active site.

Fluorescence studies on proteins, in which use is made of the emission of endogenous Tyr and Trp residues, have been widely performed to study protein structure and dynamics. Several Hcs (27–39) and one Ty (40) have been the subject of such investigations. Yet Hc or Ty protein fluorescence has never been used to study inhibitor binding. This report focuses on the fluorescence properties of the Ty from *Streptomyces antibioticus* as a function of pH and inhibitor binding. Fluoride was chosen (26) as a model compound to study the transient-state kinetics of its binding to the Ty_{met} enzyme, as well as its pH dependence. Stopped-flow fluorescence spectroscopy was used to obtain insight into the interaction of fluoride with Ty, as well as to validate the use of fluorescence quenching in studying ligand binding kinetics. The inactivation of Ty was studied at various pH values and under different conditions. To our knowledge, this is the first report on the kinetics of inhibitor binding to *oxidized* tyrosinase.

MATERIALS AND METHODS

Protein Isolation and Purification—Tyrosinase was obtained from liquid cultures of *S. antibioticus* carrying the Ty pIJ703 overexpression plasmid (25). The enzyme was purified from the growth medium according to published procedures (25). The pure enzyme was obtained as a mixture of Ty_{met}, Ty_{red}, and Ty_{oxy}, and the purity exceeded 95% in all cases as estimated by SDS-PAGE. Protein concentrations were routinely determined optically using a value of 82 mM^{-1} cm^{-1} for the extinction coefficient at 280 nm (41). The protein was stored at −80 °C at a concentration of 1 mg/ml in 100 mM P_i buffer at pH 6.8 containing 20% glycerol as a cryoprotectant. Prior to further experiments, glycerol was removed from the storage buffer by dialysis at 4 °C against 100 mM P_i at pH 6.80. The reduced enzyme was prepared by reduction with hydroxylamine as described previously (26) and used immediately.

Optical Spectroscopy—Optical measurements were performed on a PerkinElmer Life Sciences Lambda 800 spectrometer. Steady-state fluorescence measurements were performed on a PerkinElmer Life Sciences 50B fluorimeter. For recording the emission spectra, the freshly prepared enzyme was diluted in the measurement buffer immediately prior to the measurement. Anaerobic, air-saturated, or oxygen-saturated buffers were prepared by extensive bubbling with pure argon, air, or oxygen, respectively. The concentration of oxygen was assumed to be 0.27 mM for the air-saturated solutions at 20 °C and 1.32 mM for the oxygen-saturated solutions (42). For the oxygen titration experiments, small aliquots of oxygen-saturated buffer were introduced into the cuvette through an air-tight septum using a 10-μl Hamilton syringe.

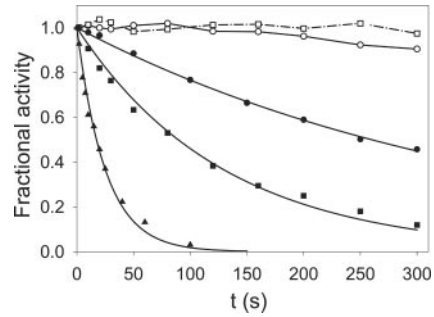

FIG. 1. **The pH-dependent inactivation of *S. antibioticus* Ty and the stabilization by halide ion.** Measurements were made at 21 °C by pH jump sequential stopped-flow where the protein was incubated at pH 3.63 (▲), pH 4.40 (■), and pH 4.85 (●) for a fixed time period and then assayed for remaining activity using 5 mM *t*-butylcatechol (see "Materials and Methods" for experimental details). *Solid lines* represent least squares fits to a mono-exponential decay function. Little inactivation could be detected when either 6 mM chloride (○) or 6 mM fluoride (□) was present in the incubation mixture at pH 4.40.

Kinetics—Stopped-flow experiments were performed using a computer-controlled Applied-Photophysics SX18MV stopped-flow system equipped with a PBP 05-109 Spectrakinetic monochromator. The system was temperature controlled at 21 °C using a Neslab RTE-111 circulation cryostat. Ty fluorescence was detected using a photomultiplier tube equipped with an optical cut-off filter of 320 nm supplied with the stopped-flow system, thus resulting in the detection of all emitted light above 320 nm. The enzyme was introduced into the reaction chamber from a stock solution kept at 4 °C. Fluoride binding traces were fitted to a single exponential decay function of the form $F_t = F_\infty + A \cdot \exp(-k_{obs} \cdot t)$, where F_t denotes the fluorescence at time t; F_∞ is the fluorescence level at completion of the binding reaction; A is the signal amplitude, and k_{obs} is the observed rate constant. The fitting was performed using the least squares fitting algorithm implemented in the stopped-flow software. The reported kinetic parameters k_{obs} and A represent the average of at least four measurements. The standard errors were less than 10% in all cases. Because fluoride ion protonates at low pH-forming HF, effective free fluoride concentrations were calculated using a value of 3.14 for the pK_a for the $HF \leftrightarrow F^- + H^+$ equilibrium (42).

RESULTS

pH-dependent Inactivation of Ty—From previous studies (26), it is known that the Ty from *S. antibioticus* is unstable at low pH. The closely related Ty from *Streptomyces glaucescens* (93% sequence identity with *S. antibioticus* Ty) is more stable in Tris·HCl buffer than in phosphate buffer, especially at the lower pH values (43). To investigate the pH stability of *S. antibioticus* Ty, and its dependence on the presence of halide ion, we performed experiments at 21 °C where the protein in 5 mM P_i at pH 7.20 was pH-jumped by rapidly mixing with 200 mM phosphate buffer at the pH of interest in 1:1 volume ratio (end buffer concentration 102.5 mM P_i) using stopped-flow. The reported pH values were measured on the final mixed solutions. The mixture was allowed to incubate for a fixed amount of time after which the solution was rapidly mixed with a 5 mM solution of *t*-butylcatechol in 5 mM P_i at the pH of the experiment. After reaching the steady-state ($t < \sim 50$ ms), linear product formation was observed. The steady-state velocity of formation of the stable reaction product *t*-butylquinone was optically measured at 410 nm for 1 s. Fig. 1 shows the normal-

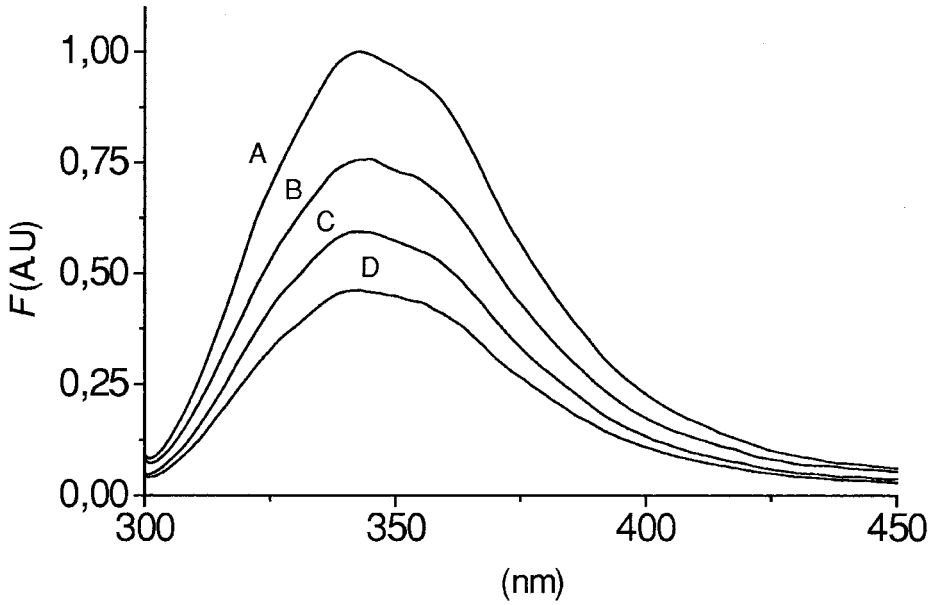

FIG. 2. **Normalized emission spectra of Ty_{red} recorded under anaerobic conditions (*A*), resting Ty (predominantly Ty_{met}, see text) under anaerobic (*B*) and aerobic conditions (*C*), and 94% Ty_{oxy} + 6% Ty_{red} (*D*).** All measurements were made in 100 mM P_i buffer at pH 6.80 and at 21 °C using an excitation wavelength of 290 nm. In all cases the total [Ty] was ~0.3 μM.

ized reaction rates *versus* incubation time under various conditions. The inactivation profiles obtained in the absence of halide (*solid data points* in Fig. 1) clearly show a pH-dependent inactivation of the protein. The data were fitted to a single exponential decay function yielding inactivation rate constants of 2.09, 0.43, and 0.16 min^{-1} at pH 3.63, pH 4.40, and pH 4.85, respectively. Curiously, little inactivation of the enzyme could be detected when 6 mM of either fluoride or chloride was present in the incubation and reaction mixtures at pH 4.40 (*open symbols* in Fig. 1). Here product formation was measured for 5 s to compensate for the inhibitory effect of halide. Apparently, the presence of halide significantly stabilizes the protein at low pH.

Fluorescence Emission of Ty in Its Three Different Oxidation States—Fluorescence emission spectra of Ty_{red} under anaerobic (Fig. 2*A*) and air-saturated (Fig. 2*D*) conditions at pH 6.80 and 21 °C are presented in Fig. 2. Whereas under anaerobic conditions only Ty_{red} is present, under air-saturated conditions the protein exists as a mixture of 94% Ty_{oxy} and 6% Ty_{red} as calculated from K_{O_2} and $[O_2]$ (see below and Fig. 3). Spectra of samples containing the resting form of the enzyme (predominantly Ty_{met}) were recorded under anaerobic (Fig. 2*B*) and aerobic (Fig. 2*C*) conditions. All species display a similar line shape for the emission band with a maximum centered at 343 ± 2 nm and a half-width of 60 ± 2 nm. Little fine structure can be distinguished, and the absence of a shoulder at 300–310 nm with all species indicates that the emission is dominated by Trp fluorescence. The partial quenching of the fluorescence by oxygen (see Fig. 2) does not exhibit Stern-Volmer characteristics (in line with what may be expected on the basis of literature data (66)) but is the result of oxygen binding (see below). When bound oxygen is displaced from Ty_{oxy} by incubation with bromide (26), an increase in fluorescence is observed in which the magnitude parallels the decrease in the optical absorption at 345 nm typical of Ty_{oxy} (data not shown). Therefore, it appears that the Ty fluorescence intensities depend on the oxidation state of the protein, the emission intensities of Ty_{red} and Ty_{oxy} differing by a factor of more than 2. The optical absorption spectra in the 250–300 nm region were identical for all three preparations (resting Ty, Ty_{red} + Ty_{oxy}, and Ty_{red}; not shown).

The relative fluorescence intensity of the resting form of the enzyme (Fig. 2, *B* and *C*) depends on the presence of oxygen in the sample. This can be explained by considering that the resting form of the enzyme contains a percentage of Ty_{red} and Ty_{oxy} in addition to a predominant amount of Ty_{met} (4, 5). Under anaerobic conditions only Ty_{met} and Ty_{red} are present, and the total fluorescence is given by Equation 1,

$$F_1 = x \cdot F_{met} + (1 - x) \cdot F_{red} \quad \text{(Eq. 1)}$$

where F_1 is the observed emission intensity; x is the fraction Ty_{met} in the sample; F_{met} is the normalized fluorescence intensity of Ty_{met}; and F_{red} is the normalized fluorescence intensity of Ty_{red}. When oxygen is present, an equilibrium between Ty_{red} and Ty_{oxy} is established, the ratio of the two species depending on the oxygen dissociation constant K_{O_2} and $[O_2]$. The total emission is then given by Equation 2,

$$F_2 = x \cdot F_{met} + (1 - x) \cdot \left(1 - \frac{K_{O_2}}{[O_2] + K_{O_2}}\right) \cdot F_{oxy} + (1 - x) \cdot \left(\frac{K_{O_2}}{[O_2] + K_{O_2}}\right) \cdot F_{red} \quad \text{(Eq. 2)}$$

From the measured emission intensities at λ_{max} and Equations 1 and 2, the fraction of Ty_{met} as well as the relative Ty_{met} emission intensity can be calculated according to the following Equations 3 and 4,

$$x = \frac{(F_1 - F_2)K_{O_2} + (F_1 - F_2 - F_{red} + F_{oxy})[O_2]}{(F_{oxy} - F_{red})[O_2]} \quad \text{(Eq. 3)}$$

and

$$F_{met} = \frac{(F_{red}F_1 - F_{red}F_2)K_{O_2} + (F_{oxy}F_1 - F_{red}F_2)[O_2]}{(F_1 - F_2K_{O_2} + (F_1 - F_2 - F_{red} + F_{oxy})[O_2]} \quad \text{(Eq. 4)}$$

By using 0.27 mM for $[O_2]$, 16.5 μM for K_{O_2} (see below and Fig. 3), 1 for F_{red}, 0.41 for F_{oxy} (see below), and the measured intensities F_1 and F_2, amounting to 0.76 and 0.60, respectively, a value of 0.71 is obtained for the fraction Ty_{met} in the sample (x) and a value of 0.66 for the fractional emission intensity F_{met} relative to that of Ty_{red}. In a resting Ty sample in air-saturated buffer at pH 6.80 and 21 °C, it is calculated that Ty_{oxy} and Ty_{red} contribute a fraction of 0.21 to the total fluorescence, whereas 0.79 of the emission originates from the Ty_{met} species. We found the fraction of Ty_{met} in our fresh preparations to be constant under the used experimental conditions.

Oxygen Binding—We have studied the steady-state binding of molecular oxygen to Ty_{red}, rendering Ty_{oxy}, by following the

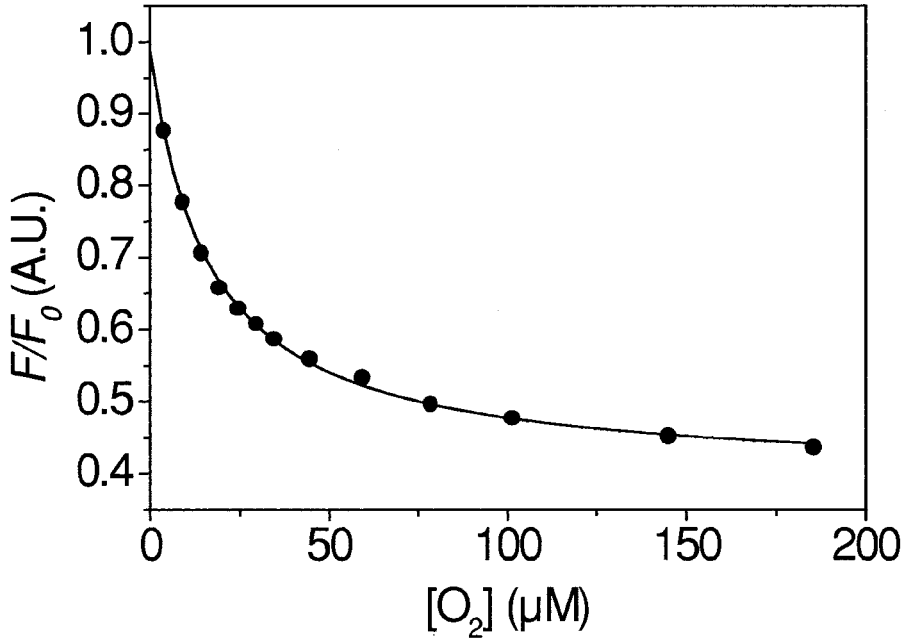

FIG. 3. **The binding of molecular oxygen to Ty_{red} rendering Ty_{oxy}, at pH 6.80 and 21 °C measured by following the changes occurring in the endogenous Ty fluorescence upon titrating an anaerobic solution of Ty_{red} (0.5 μM) with a solution saturated with O_2 ($[O_2]$ = 1.32 mM).** The *solid line* represents the best fit to Equation 5 with K_d 16.5 ± 1.2 μM and $f_{q(max)}$ 0.59. The conditions are as follows: 100 mM P_i, λ_{ex} 290 nm, and λ_{em} = 345 nm.

changes occurring in the Ty Trp fluorescence as described above (λ_{ex} 290 nm and λ_{em} 345 nm). For this, 3.0 ml of a freshly prepared anaerobic solution of 0.1 μM Ty_{red} in 100 mM P_i at pH 6.80 was introduced in a sealed 3.5-ml quartz cuvette, after which this solution was titrated with microliter amounts of a 100 mM P_i buffer saturated with oxygen. The fluorescence emission intensity at 345 nm at given $[O_2]$ was measured using a 5-s instrument integration time. The resulting measured intensities, expressed as F/F_0 *versus* $[O_2]$, are represented in Fig. 3. The data could be accurately fitted assuming the binding of a single oxygen using Equation 5,

$$\frac{F}{F_0} = 1 - \frac{f_q \cdot [L]}{[L] + K_d} \qquad \text{(Eq. 5)}$$

where F denotes the observed fluorescence intensity; F_0 denotes the fluorescence intensity in the absence of ligand; [L] denotes the ligand concentration; K_d denotes the dissociation constant for ligand L; and f_q denotes the fractional decrease in fluorescence upon complete saturation with the ligand, *i.e.* at $[L] \gg K_d^{app}$. Values of 16.5 ± 1.2 μM for the oxygen dissociation constant and of 0.59 for f_q were obtained. The latter value means that the fluorescence intensity of the Ty_{oxy} species amounts to 0.41 of the Ty_{red} fluorescence intensity.

The pH Dependence of Ty Fluorescence—Because we found that Ty is unstable at low pH (see Fig. 1), we measured the pH dependence of Ty fluorescence by pH jump stopped-flow at a time scale where the protein has not decayed to any measurable extent. For this, we rapidly mixed an ~2 μM Ty solution in 1 mM P_i at pH 7.20 with a 200 mM air-saturated P_i buffer at the pH of interest in a 1:1 volume ratio ([Ty] ~1 μM; 3.8 < pH < 9.0). The fluorescence level was then measured for 0.25 s. The measurements were performed with three Ty preparations: resting Ty (71% Ty_{met}, 27% Ty_{oxy}, and 2% Ty_{red}), reduced Ty (94% Ty_{oxy} and 6% Ty_{red}), and resting Ty in the presence of 100 mM fluoride. In the time period of the measurement, the fluorescence was stable. The actual pH values were measured on the mixed solutions. The obtained emission intensity data, expressed as the fractions of emission intensity relative to that of Ty_{red}, are presented in Fig. 4. For the reduced sample containing Ty_{oxy} and Ty_{red}, there is no detectable pH dependence of the emission intensity. For the resting Ty sample, the emission intensity decreases at low pH. Because the emission of the reduced sample was not sensitive to the pH, the observed variation in emission must be due to changes in the contribution of Ty_{met}. Accordingly, the experimental data were corrected for the contribution of Ty_{oxy} and Ty_{red} to the emission (0.21 of F_0 at pH 6.80) and normalized using the calculated value of F_{met} of 0.66 at pH 6.80. The corrected data are plotted in Fig. 4. The Ty_{met} emission data can be interpreted by assuming that the fluorescence level is under control of a single acid/base equilibrium according to Equation 6,

$$F_{obs} = \frac{F_A \cdot [H^+] + F_B \cdot K_a}{[H^+] + K_a} \qquad \text{(Eq. 6)}$$

where F_{obs} denotes the observed fluorescence level at given pH; F_A denotes the fluorescence level of the acidic form of the protein, and F_B the fluorescence level of the basic form of the protein. Fitting the data to Equation 6 yields a pK_a value of 4.5 ± 0.1 and a value of 0.42 for F_A, *i.e.* the relative fluorescence level of the acidic form of the enzyme relative to the fluorescence level of Ty_{red}. Remarkably, the fluorescence level of resting Ty + fluoride is independent of the pH between pH 3.75 and pH 6.25. Here a $[F^-]$ of 100 mM was present in both the enzyme and the buffer solution. At this $[F^-]$, the Ty_{met} enzyme can be considered to be fully saturated with F^- at all pH values used in the experiment, whereas fluoride does not interact with Ty_{red} and Ty_{oxy} (see Ref. 26 and see below). Depending on the pH, the relative fluorescence intensities of Ty_{met} and $Ty_{met}F$ differ significantly, showing that the protein fluorescence can be exploited as a probe to study the fluoride binding.

Stopped-flow Studies of Fluoride Binding—We studied the binding of fluoride to Ty_{met} and its pH dependence between pH 4.0 and pH 7.9 by using stopped-flow fluorescence spectroscopy under pseudo first-order conditions ($[F^-] \gg [Ty_{met}]$). Representative fluoride binding traces obtained by mixing ~2.5 μM resting Ty with various $[F^-]$ (0–120 mM) at pH 6.80 in 1:1 volume ratio and 21 °C are represented in Fig. 5*A*, where a decrease in fluorescence is observed upon binding of F^-. At all pH values and at all $[F^-]$, traces could be fitted with good accuracy to a mono-exponential decay function, yielding values for the apparent binding rate (k_{obs}) and signal amplitude (A) at each $[F^-]$. At pH 6.80, no change in protein fluorescence was observed when 50 mM fluoride was mixed with Ty_{oxy} and Ty_{red}, showing that the observed kinetics were solely due to the

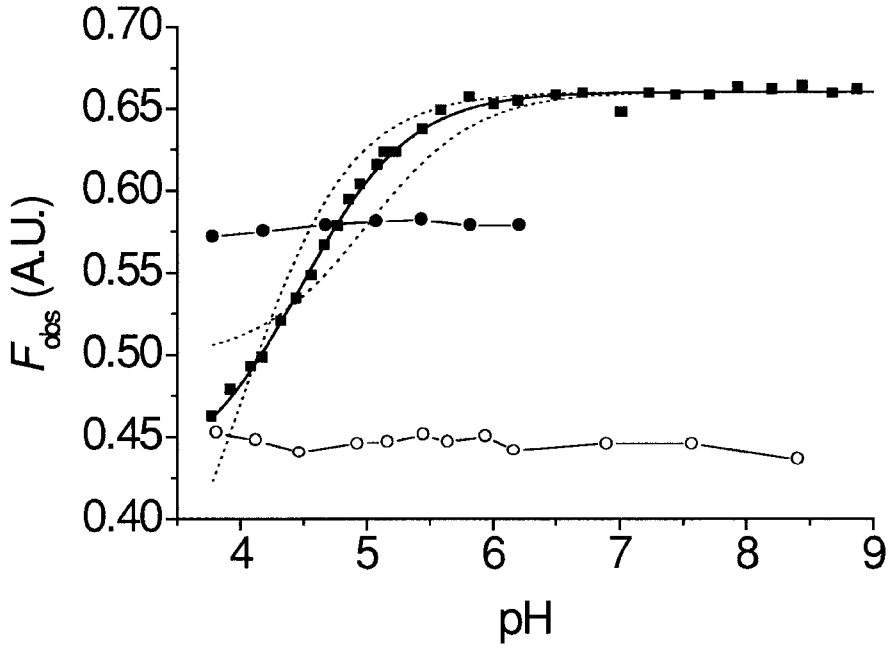

FIG. 4. **The pH dependence of the fluorescence emission intensity of resting Ty (71% Ty_{met}, 27% Ty_{oxy}, and 2% Ty_{red}) (■), resting Ty + 100 mM fluoride (●), and reduced Ty (94% Ty_{oxy} and 6% Ty_{red}) (○).** Measurements were made by pH jump stopped-flow as described in the text. For Ty_{met}, the data were fit to Equation 6 with a pK_a value of 4.50. For comparison, best fits to the data only varying F_A in Equation 6 and using fixed pK_a values of 4 and 5 are also included in the figure (*dotted lines*). The conditions are as follows: 100 mM P_i, 21 °C, λ_{ex} 285 nm, λ_{em} > 320 nm and a total [Ty] of ~1 μM.

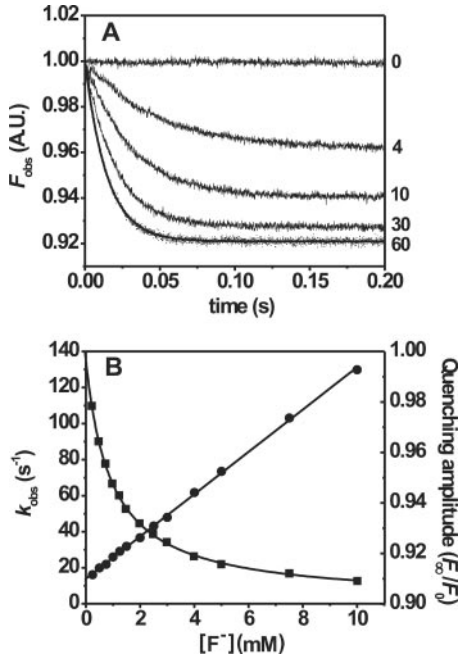

FIG. 5. **The kinetics of fluoride binding to Ty_{met}.** *A*, stopped-flow fluorescence traces of fluoride binding obtained by mixing 2.5 μM resting Ty in air-saturated 100 mM P_i at pH 6.80 with solutions containing various concentrations of fluoride made up in the same buffer. The fluoride concentrations (in mM) indicated with each trace represent end concentrations in the observation cell. Data could be fitted to single exponential decay functions (as indicated for the trace with [F^-] = 60 mM) yielding values for the observed binding rate k_{obs} and the fractional fluorescence quenching amplitude F_∞/F_0 at each [F^-]. *B*, observed binding rates k_{obs} (●) and the fractional fluorescence quenching amplitudes F_∞/F_0 (■) *versus* [F^-] measured at pH 6.03. For k_{obs} *versus* [F-], the *solid line* represents a linear fit of the data (Equation 7) with k_{on}^{app} 11.7 mM^{-1} s^{-1} and k_{off} 13.9 s^{-1}. For F_∞/F_0 *versus* [F^-], the *solid line* represents a fit to Equation 5 with K_d^{app} = 0.90 mM and f_q = 0.10. In all measurements, the conditions are as follows: 100 mM P_i, 21 °C, λ_{ex} 285 nm and λ_{em} > 320 nm. Note that *A* and *B* refer to experiments performed at different pH values.

interaction of fluoride with Ty_{met}. This is in line with an earlier observation that the addition of fluoride to a solution of Ty_{oxy} does not influence the position or the intensity of the LMCT transition of Ty_{oxy} (26).

The plots of k_{obs} *versus* [F^-] at given pH were linear in all cases, in agreement with a two-state binding scheme where a single fluoride ion binds to the enzyme. Representative data obtained at pH 6.03 are shown in Fig. 5*B*. The apparent first-order fluoride binding rate (k_{on}^{app}) and the $Ty_{met}F$ fluoride dissociation rate constant (k_{off}) can be determined from the slope and intercept of k_{obs} *versus* [F^-], according to Equation 7 (44),

$$k_{obs} = k_{on}^{app}\cdot[F^-] + k_{off} \qquad \text{(Eq. 7)}$$

At pH 6.03 (Fig. 5*B*), values of 11.7 mM^{-1} s^{-1} and 13.9 s^{-1} for the k_{on}^{app} and k_{off} were obtained, respectively. The signal amplitudes, expressed as F_∞/F_0, are also represented in Fig. 5*B*. As with the k_{obs} values, the data are in agreement with the binding of a single fluoride ion and were fitted to Equation 5 with L = F^-. For the data at pH 6.03 in Fig. 5*B*, values of 0.90 mM and 0.10 were obtained for K_d^{app} and f_q, respectively.

Because the protein appeared unstable at the lower pH values (see Fig. 1), the fluoride binding at the two lowest pH values was studied using pH jump sequential stopped-flow where an ~5 μM protein solution in 1 mM P_i at pH 7.2 was mixed with 200 mM P_i buffer at the pH of interest, after which the solution was allowed to equilibrate for 0.5 s. The resulting solution was then mixed with a fluoride solution in 100 mM P_i at the pH of the experiment after which the fluorescence trace was recorded. The reported pH values were measured in the final mixed solutions. The sequential flow method gave identical results to those obtained through single mixing experiments at pH 6.0 as used for the higher pH values. At pH 4.04, an increase in fluorescence was observed, in agreement with the pH dependence of native Ty_{met} and $Ty_{met}F$ fluorescence as depicted in Fig. 4 and indirectly illustrating the reversibility of the pH dependence of the native Ty_{met} emission. We did not measure the fluoride binding kinetics in the pH range of 4.2–5.0, because in this region the fluorescence levels of the native and the fluoride-bound Ty_{met} do not differ enough (see Fig. 4). The log values of the obtained k_{on}^{app} values are represented in Fig. 6. It appears that the log(k_{on}^{app}) is directly proportional to the pH in the pH range 6–8, whereas it levels off at pH < 5.5. This can be explained by Scheme 1, where fluoride ion only binds to the acidic form of the enzyme, as was proposed earlier on the basis of paramagnetic NMR and fluoride inhibition studies (26). There it was shown that the pH dependence of

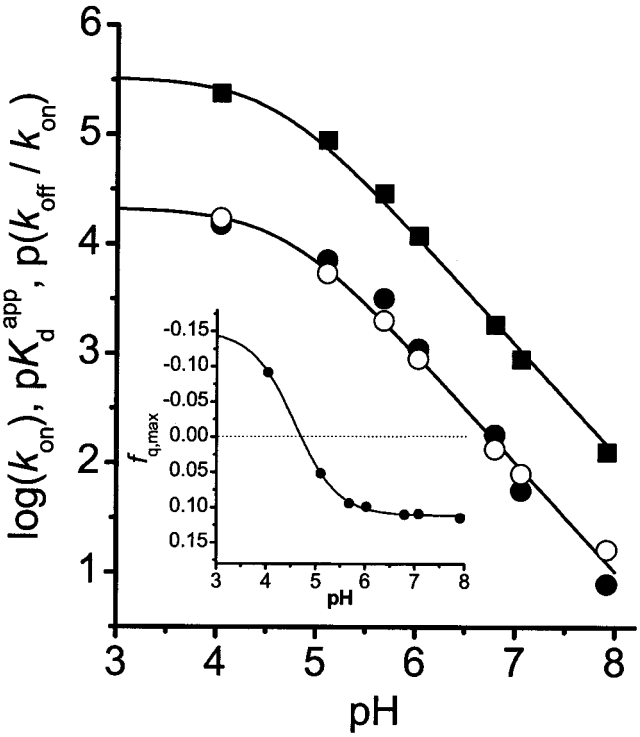

FIG. 6. **The pH dependence of the kinetic parameters of fluoride binding to Ty_{met} showing the apparent association rates k_{on}^{app} (■) and the apparent dissociation constants K_d^{app} determined from amplitude data (●) and from k_{off}/k_{on} (○) *versus* the pH.** For k_{on}^{app}, the *solid line* represents a fit to Equation 8 with pK_a = 4.57 and $k_{on} = 3.3 \cdot 10^5$ M^{-1} s^{-1}. For K_d^{app} and k_{off}/k_{on}, the *solid line* was obtained from fitting the K_d^{app} data with a pK_a value of 4.68 and K_d = 48 μM. The *inset* shows the pH dependence of the fractional change in Ty_{met} fluorescence $f_{q(max)}$ upon complete saturation with fluoride as obtained from stopped-flow F_∞/F_0 *versus* [F$^-$] data. The *solid line* represents a fit of the data with a pK_a value of 4.57. In all measurements, the conditions were 100 mM P_i, 21 °C, λ_{ex} 285 nm and λ_{em} > 320 nm.

chloride binding to Ty_{met} shows analogous behavior to that of fluoride binding. It is therefore unlikely that the observed pH dependence of the apparent k_{on} for fluoride originates from the exclusive binding of HF (pK_a 3.14), because HCl (pK_a −7) occurs fully dissociated in the pH range of the experiment.

The finding that the fluoride binding traces follow monoexponential behavior, as well as linear dependence of k_{obs} on [F$^-$] at all pH values, shows that the pH-dependent step is fast in comparison with the fluoride binding step. In that case, the measured k_{on}^{app} values are proportional to the fraction of Ty_{met} that is in the low pH form (44) according to Equation 8,

$$k_{on}^{app} = k_{on} \frac{[H^+]}{[H^+] + K_a} \qquad \text{(Eq. 8)}$$

Fitting the data in Fig. 6 to this function yielded a pK_a of 4.6 ± 0.1, which is within error of the pK_a found for the pH dependence of native Ty_{met} fluorescence as depicted in Fig. 4. The fit also yielded an estimate for the k_{on} of fluoride binding to the low pH form of the enzyme, amounting to $(3.3 \pm 0.7) \cdot 10^5$ M^{-1} s^{-1}. The determined values for k_{off} are much less dependent on the pH, in agreement with the mechanism in Scheme 1 (44), and varied between 8 s^{-1} and 16 s^{-1} without showing a clear correlation with the pH (not shown). From the k_{on} value and the value of k_{off} determined at the lowest pH used (pH 4.04; 12.3 ± 0.8 s^{-1}), the K_d for fluoride for binding to the low pH enzyme can be estimated from the relation $K_d = k_{off}/k_{on}$, amounting to 37 ± 8 μM.

The values for the apparent dissociation constants K_d^{app} as determined from signal amplitudes and Equation 5 follow similar behavior as the k_{on}^{app} values, as expected from the relative insensitivity of k_{off} to the pH, as shown in Fig. 6. Here the data could be fitted to Equation 8 (with k_{on} substituted for by K_d) with a pK_a value of 4.7 ± 0.2, whereas the dissociation constant for the $Ty_{met}F$ complex was estimated at 54 ± 22 μM by extrapolation to low pH. As depicted in Fig. 6, there is good agreement between the K_d^{app} values determined from amplitude data and those calculated from $K_d^{app} = k_{off}/k_{on}^{app}$. From the latter data, values of 4.7 ± 0.2 for the pK_a and 48 ± 10 μM for the K_d for the $Ty_{met}F$ complex were obtained.

The pH dependence of the determined f_q values, *i.e.* the fractional changes in fluorescence upon complete saturation of Ty_{met} with fluoride, is shown in Fig. 6. The obtained values are in good agreement with the data obtained for the pH dependence of the Ty_{met} and $Ty_{met}F$ fluorescence intensities as described above (Fig. 4). The data could be fit assuming that f_q is dependent on a single acid/base equilibrium, yielding an estimate for the pK_a value of 4.6 ± 0.1.

DISCUSSION

Ty Fluorescence Properties and Emission Quenching—Ty from *S. antibioticus* contains 12 tryptophans and 6 tyrosines on a total of 272 amino acids. Consistent with the Trp/Tyr ratio and the excitation wavelength employed, all Ty species (Ty_{met}, Ty_{oxy}, and Ty_{red}) display emission spectra dominated by Trp fluorescence. The positions of the emission maxima (343 ± 2 nm for all species) are the highest reported for a type 3 copper protein and indicate that a significant fraction of the Trp residues is exposed to the solvent. As was found earlier for several hemocyanins (27–39) and *Neurospora crassa* tyrosinase (40), it appears that the Ty fluorescence emission intensities are markedly sensitive to the oxidation state of the dinuclear copper center; the emission quantum yields of Ty_{red} and Ty_{oxy} differ by more than a factor of 2.

The mechanism of quenching has not been unambiguously established for any Hc or Ty. For Ty_{oxy}, the fluorescence quenching possibly occurs through Förster energy transfer because the Ty emission spectrum (λ_{max} = 343 nm) overlaps with the strong LMCT transition absorption band characteristic of Ty_{oxy} (ϵ_{345} = 18.5 mM^{-1} cm^{-1}). The energy transfer mechanism may also contribute to the fluorescence quenching in the Ty_{met} species considering the weak LMCT between the Cu(II) and the ligand nitrogens in the emission region ($\epsilon_{320} \sim 2$ mM^{-1} cm^{-1}). The relatively high quantum yield of the Ty_{red} species may be due to the absence of Förster quenching consistent with the absence of absorption bands in the emission region. The fluorescence changes that occur upon fluoride binding to Ty_{met} might be associated with electronic changes at the active site. To elucidate the mechanism of quenching, further study is needed. For the purpose of the present investigations it is sufficient to note that the large differences between the emission intensities of the various Ty species can be used as a sensitive probe of ligand binding and of interconversion between the Ty redox states.

The Composition of Resting Ty and Oxygen Binding—The resting form of the enzyme in our preparations is a mixture of oxidized (Ty_{met}) and reduced (Ty_{red} + Ty_{oxy}) enzyme. From the fluorescence data in Fig. 2, it was possible to calculate that 71% of the enzyme occurs in the oxidized form, whereas the remainder is a mixture of Ty_{oxy} and Ty_{red}, the ratio of the latter two species depending on the concentration of oxygen in the sample. In the literature, it is usually reported that more than 85% of the enzyme occurs in the oxidized form in resting Ty (5). The ratio of oxidized and reduced Ty in resting preparations determines in part the length of the lag phase observed in the conversion of monophenolic compounds (5). The stable percentage of Ty_{met} in resting preparations may reflect a natural

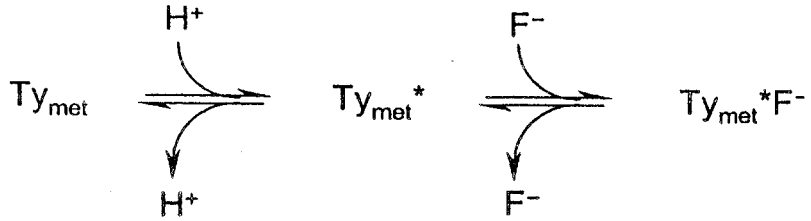

SCHEME 1

equilibrium between the three Ty species present in solution. Establishment of this equilibrium may be connected with the dissociation of peroxide from Ty_{oxy} resulting in the formation of Ty_{met}, as observed for *N. crassa* Ty (45). This would be consistent with the observed slow decay of Ty_{oxy} to Ty_{met} in fresh preparations of *S. antibioticus* Ty_{red}.[2]

The large difference between the Ty_{red} and Ty_{oxy} quantum yield has been used to study the binding of molecular oxygen to the reduced enzyme (Fig. 3). The obtained dissociation constant for the oxygenated Ty complex of 16.5 μM is lower than that reported for mushroom Ty (47 μM (46)) and *Octopus vulgaris* hemocyanin (90 μM (47)). This higher affinity of Ty_{red} for oxygen may reflect adaptation to an oxygen-poor environment, as experienced by soil bacteria like *Streptomyces* in their natural environment.

The Kinetics of Fluoride Binding—Recently a structural and mechanistic study of the interaction of halide ions with *S. antibioticus* Ty was reported (26). The interaction of fluoride with Ty was the most extensively studied. In contrast to the other halides, fluoride solely interacts with the Ty_{met} form of the protein and acts as a simple competitive inhibitor in the conversion of L-DOPA, whereas the other halides interact with both Ty_{met} and Ty_{red}.

It appears that the Ty_{met} and the $Ty_{met}F$ fluorescence emission levels differ significantly and that this difference is dependent on the pH as depicted in Figs. 4 and 6 (*inset*). This feature has been exploited in studying the transient state kinetics of fluoride binding to Ty_{met} by stopped-flow fluorescence spectroscopy. All data are in agreement with the binding of a single fluoride ion and can be explained by adopting a simple binding mechanism. Likewise, titrations of Ty_{met} with fluoride followed by ^1H paramagnetic NMR (26) could also be explained by assuming a binding mechanism where a single fluoride ion binds to Ty_{met}. From that work, it was proposed that a single halide ion binds to Ty_{met} at the Cu_2 bridging position. The findings presented here are consistent with this hypothesis. The presence of a Cu_2 bridging ligand in Ty_{met} is also corroborated by extended x-ray absorption fine structure studies on *S. antibioticus* Ty[3] and oxidized catechol oxidase (48), indicating 3N/1O coordination for each copper ion, as well as with the crystal structure of oxidized sweet potato catechol oxidase, where a single Cu_2 bridging ligand (possibly chloride) was identified in the electron density map upon refinement (12, 49).

At pH 6.80, the K_d^{app} value as determined from amplitude data is 6.0 mM, whereas the K_d^{app} amounts to 7.4 mM by using the relation $k_{off}/k_{on}^{app} = K_d^{app}$. These values, taking into account the notable pH sensitivity of the fluoride binding, compare reasonably well with the competitive inhibition constant for fluoride of 11.8 mM obtained at the same pH and temperature and the dissociation constant of 5.1 mM for the fluoride Ty_{met} complex determined at pH 7.06 and 4 °C by using paramagnetic NMR (26). The relatively low value of the fluoride dissociation rate, k_{off} (13.7 ± 0.5 s^{-1} at pH 6.80), is in agreement with the previous finding that fluoride is in slow exchange on the (paramagnetic) NMR shift time scale (26). The observation that no changes in fluorescence are observed when Ty_{red} or Ty_{oxy} are mixed with 50 mM fluoride at pH 6.80 is in agreement with the previous finding that fluoride solely interacts with the Ty_{met} protein.

The pH Dependence of the Kinetic Parameters of Fluoride Binding to Ty_{met}—It appears that the fluoride binding to Ty_{met} is strongly dependent on the pH, as was observed earlier by paramagnetic NMR of Ty_{met} and its halide-bound species and by kinetic studies of the inhibition of the conversion of L-DOPA by halide ion (26). The latter data could be explained by assuming that the halide binding to Ty_{met} is under control of a single acid/base equilibrium where the ion only binds to the acidic form of Ty_{met}. Due to the experimental limitations imposed by the instability of Ty_{met} at low pH and the relatively long experimental times required, it was only possible to determine an upper limit for the pK_a of this acid/base equilibrium ($pK_a < 5.5$). By using the faster method of stopped-flow fluorimetry, the problem of protein instability has been circumvented in the present study.

The kinetic parameters of fluoride binding corroborate the earlier finding that fluoride ion only binds to the acidic form of the enzyme as witnessed by the pH dependence of k_{on}^{app} and K_d^{app} (Fig. 6) and the relative insensitivity of k_{off} to the pH. The data obtained for the pH dependence of k_{on}^{app} could be fitted using a pK_a value of 4.6 ± 0.1, which is equal, within the experimental error, to the pK_a values obtained from the pH dependence of K_d^{app} and k_{off}/k_{on} (4.7 ± 0.2). Similar pK_a values are obtained from the pH dependence of the Ty_{met} fluorescence (Fig. 4; pK_a 4.5 ± 0.1) and of f_q, *i.e.* the fractional changes in Ty_{met} emission upon complete saturation with fluoride (Fig. 6; pK_a 4.6 ± 0.1). This provides a total of 5 pK_a values, the average amounting to 4.59 ± 0.05.

Fluoride Replaces Hydroxide as the Bridging Ligand in Ty_{met}—Fluoride is known to inhibit many metalloenzymes (*e.g.* superoxide dismutase (50), urease (51), laccase (52), peroxidase (53), and enolase (54)), often with apparent inhibition constants in the micromolar to millimolar range. In most cases, the fluoride binding is pH-dependent, and it is thought that fluoride replaces a metal-bound hydroxide ion or water ligand. The results presented here suggest that the same occurs with Ty. We propose that the pH dependence of fluoride binding derives from the pH-dependent dissociation of Cu_2 bridging hydroxide according to the mechanism outlined in Scheme 2. Direct dissociation of OH^- or dissociation of water after protonation of the bound hydroxide are indistinguishable at present. As established earlier on the basis of paramagnetic NMR of Ty_{met} (26), it can be excluded that the pH dependence of fluoride binding results from a protonation and subsequent dissociation of a coordinating histidine residue at low pH. Such a mechanism was proposed earlier to explain the pH dependence of halide inhibition (22, 55, 56). A pH-dependent dissociation of Cu_2 bridging hydroxide has been shown to occur for several small dinuclear copper model compounds (57–59). Therefore,

[2] A. W. J. W. Tepper, L. Bubacco, and G. W. Canters, unpublished data.

[3] L. Bubacco *et al.*, manuscript in preparation.

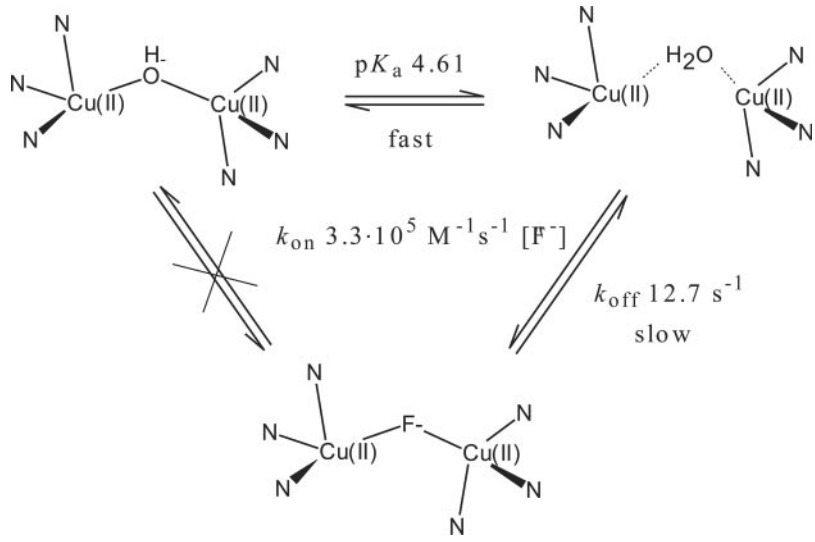

SCHEME 2. **Proposed mechanism of fluoride binding to Ty_{met} and kinetic parameters of the process.** Copper bridging hydroxide in the native Ty_{met} dissociates or protonates at low pH, rendering the bridging position available for fluoride to bind. The solvent water in the low pH form of the oxidized enzyme is drawn putatively. The depicted pK_a value for the hydroxide dissociation/protonation process is the average of that found from the pH dependence of k_{on} (Fig. 6), K_d^{app} (Fig. 6), k_{off}/k_{on} (Fig. 6), the pH dependence of f_q values (*inset*, Fig. 6), and the fluorescence emission quantum yield of native Ty_{met} (Fig. 4). The reported fluoride association constant k_{on} was obtained from fitting the data in Fig. 6, whereas the reported dissociation rate constant k_{off} is the average of the k_{off} values determined at 6 pH values.

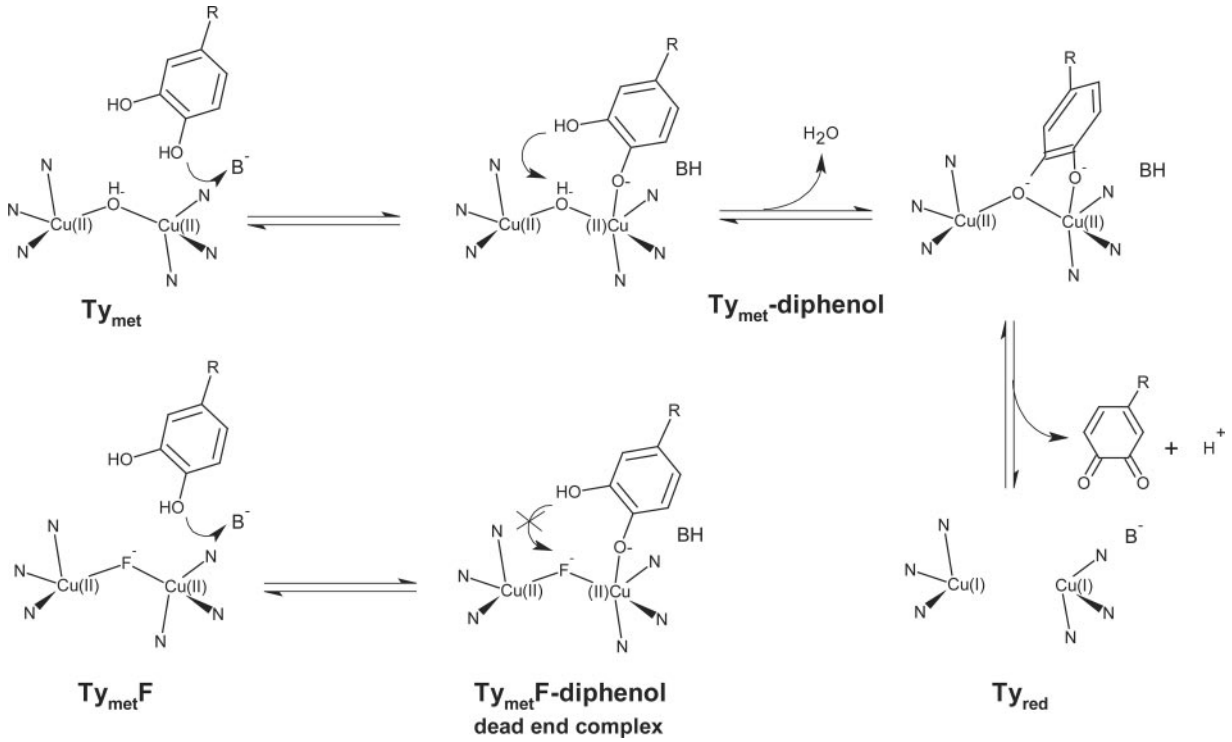

SCHEME 3. **Proposed mechanism of the diphenolase reaction of Ty_{met}.** Upon entering the binding cavity one of the phenol groups of the substrate gives off a proton to a nearby base (B^-) and binds to one of the copper ions in the active site. Binding to the Cu(II) leads to a slight charge redistribution in the ring by which the remaining OH group on the ring becomes less electronegative and dissociation of the second proton is promoted. This proton binds to the bridging OH^- which then leaves the site in the form of a water molecule allowing the deprotonated oxygen of the ring to take up the bridging position between the two copper ions. Reduction of the two copper ions and dissociation of the quinone leaves the two copper ions in the reduced three coordinated form, a step with a high driving force (61). The analogous situation with F^- as the bridging ligand is depicted in the *lower left-hand part* of the scheme. The low pK_a of the fluoride prevents dissociation of a proton in the second binding step of the substrate, and a dead-end complex is formed.

pK_a values between 4.0 and 5.5 have been obtained for the dissociation process, comparable with the average pK_a of 4.59 ± 0.05 found in the present case. This low pK_a value can be ascribed to the charge of the two copper ions and the relatively low basicity of the coordinating histidine ligands. The linear dependence of k_{obs} on [F^-] at all pH values implies that both the hydroxide dissociation and association processes are much faster than the corresponding steps for fluoride.

The pH Dependence of the Ty_{met} Fluorescence Emission—The pH dependence of the fluorescence emission intensity of Ty was studied under various conditions by pH jump stopped-flow fluorimetry (Fig. 4). It appeared that the emission level of the Ty_{met} enzyme is dependent on an acid/base equilibrium with an apparent pK_a value of 4.5 ± 0.1, which is identical to the experimental pK_a values found for fluoride binding. It was estimated that the low pH form of Ty_{met} has an emission intensity ~0.7 that of the high pH form. A pH dependence of the emission intensity is not observed for Ty_{red} or Ty_{oxy} or for Ty_{met} bound with fluoride. This strongly suggests that the pH dependence of Ty_{met} emission is associated with pH-dependent changes occurring directly at the oxidized dinuclear copper center. If it would reflect, for example, a protonation of a carboxylic acid residue in close vicinity to a fluorescent Trp or pH-dependent changes in protein structure, a pH dependence

of the emission would also be expected for the other species, contrary to what is observed. Thus, in view of the current proposal that bridging hydroxide dissociates at low pH, it is likely that this process is responsible for the decrease in quantum yield. We note that this would lead to loss of the antiferromagnetic coupling between both copper ions, as has been shown to occur for Cu_2 model compounds. Therefore, a marked change in paramagnetism is expected upon loss of the bridging ligand, which could be related to the lower quantum yield of the enzyme at low pH.

The Role of the Bridging Ligand in the Diphenolase Mechanism—The role of bridging hydroxide in the oxidation of diphenols has yet to be established. Previously it was shown that halide is displaced from Ty_{met} if inhibitors that mimic the transition state (*e.g.* mimosin, Kojic acid) are bound to the enzyme. On this basis a model for diphenol coordination was proposed whereby one of the phenolic oxygens bridges the two copper ions by displacing the bridging hydroxide that is present in native Ty_{met} (26). The displacement of an equatorial water ligand by bidentate ligands has also been shown to occur for half-oxidized Ty ($Ty_{half\text{-}met}$) by means of pulsed EPR spectroscopies (60, 61). For oxidation of a diphenolic substrate to proceed, the diphenol must lose two protons in the process. Thus, the hydroxide could function as the proton acceptor for one of the phenolic protons in the conversion of diphenols as outlined in Scheme 3. The observation that catalysis does not proceed when fluoride bridges the copper ions, its size and charge being similar to hydroxide notwithstanding, would be in agreement with this hypothesis. Still, we cannot exclude that changes in the redox potential(s) of the system upon changing the bridging ligand, as demonstrated for Cu_2 model complexes (62), might also be responsible for the absence of catalytic activity in halide-bound Ty_{met}.

Enzyme Inactivation and the Protective Effect of Halide Ion—As depicted in Fig. 1, Ty is rapidly inactivated at low pH where the rate of inactivation is pH-dependent. It is likely that this inactivation originates from the loss of the Cu_2 bridging hydroxide in Ty_{met}, *i.e.* one negative charge, at low pH, which illustrates the importance of charge compensation in the stability of protein metal sites. Support for this is provided by the observation that protein inactivation proceeds much slower when fluoride or chloride, which are able to substitute for OH^- and therefore conserve the native coordination number and charge, is present in solution. Furthermore, the stabilizing effect of fluoride and the finding that this ion specifically interacts with Ty_{met} suggest that the inactivation is specifically due to the decay of the Ty_{met} form. Ty_{oxy} and Ty_{red} do not seem to be susceptible to rapid protein inactivation, providing further support for the loss of bridging OH^- as the cause for the inactivation of Ty_{met}.

Physiological Relevance of the Halide Inhibition—It has been proposed that the large variations in the extent of pigmentation in different human skin types originate from variations in the melanosomal pH (63–65). These pH variations would influence the Ty activity, a lower pH value being associated with a lower Ty activity and, thus, with a lower pigmentation level. For *S. antibioticus* Ty, we found that the apparent chloride inhibition constant (0.16 M at pH 6.80) is in the order of physiological chloride concentrations (5–200 mM). Similar values for the apparent chloride inhibition constant, as well as strong pH dependence of halide inhibition, have been found for other Tys (22, 55, 56). Thus, depending on the $[Cl^-]$ to K_I ratio, a significant fraction of the enzyme may exist as the inactive chloride-bound form at low pH, which is, however, protected from protein degradation. This might provide an explanation of the sensitivity of Ty activity to melanosomal pH.

Conclusion—In conclusion, the use of Ty fluorescence quenching as a probe in studying the kinetics of fluoride binding to the type 3 copper center yields results that are consistent with previously obtained kinetic and spectroscopic data. The method provides a direct spectroscopic probe of fluoride binding to Ty_{met}. Stopped-flow fluorimetric experiments can be performed with high sensitivity and speed, thereby avoiding the need for large amounts of protein and the experimental difficulties arising from the intrinsic instability of the enzyme, the latter being important especially at the lower pH values. The quenching of the Ty_{met} emission upon the binding of exogenous ligands may not be limited to the Ty from *S. antibioticus*; a similar behavior for other type 3 copper proteins would allow for a systematic comparison of the ligand binding properties of different tyrosinases, catechol oxidases, and hemocyanins, potentially providing further insight into the mechanisms that underlie the variation in the functionality of these proteins. The notable sensitivity of the Ty emission quantum yield to the state of the type 3 copper center holds promise for further studies. For example, the Ty fluorescence could be used to study the kinetics of the conversion of monophenolic and diphenolic substrates. The thermodynamics and pH dependence of inhibitor binding could be investigated by stopped-flow fluorescence kinetics. A systematic investigation of the binding kinetics of a range of organic inhibitors to Ty_{met} is underway.

REFERENCES

1. Oetting, W. S., and King, R. A. (1994) *J. Investig. Dermatol.* **103,** S131–S136
2. Oetting, W. S. (2000) *Pigm. Cell Res.* **13,** 320–325
3. van Gelder, C. W., Flurkey, W. H., and Wichers, H. J. (1997) *Phytochemistry* **45,** 1309–1323
4. Solomon, E. I., Sundaram, U. M., and Machonkin, T. E. (1996) *Chem. Rev.* **96,** 2563–2605
5. Sánchez-Ferrer, A., Rodríguez-López, J. N., García-Cánovas, F., and García-Cánovas, F. (1995) *Biochim. Biophys. Acta* **1247,** 1–11
6. Seo, S. Y., Sharma, V. K., and Sharma, N. (2003) *J. Agric. Food Chem.* **51,** 2837–2853
7. Decker, H., Dillinger, R., and Tuczek, F. (2000) *Angew. Chem. Int. Ed. Engl.* **39,** 1587–1591
8. Bubacco, L., Salgado, J., Tepper, A. W., Vijgenboom, E., and Canters, G. W. (1999) *FEBS Lett.* **442,** 215–220
9. Cuff, M. E., Miller, K. I., van Holde, K. E., and Hendrickson, W. A. (1998) *J. Mol. Biol.* **278,** 855–870
10. Hazes, B., Magnus, K. A., Bonaventura, C., Bonaventura, J., Dauter, Z., Kalk, K. H., and Hol, W. G. J. (1993) *Protein Sci.* **2,** 597–619
11. Magnus, K. A., Hazes, B., Ton-That, H., Bonaventura, C., Bonaventura, J., and Hol, W. G. (1994) *Proteins* **19,** 302–309
12. Klabunde, T., Eicken, C., Sacchettini, J. C., and Krebs, B. (1998) *Nat. Struct. Biol.* **5,** 1084–1090
13. Decker, H., and Tuczek, F. (2000) *Trends Biochem. Sci.* **25,** 392–397
14. Gerdemann, C., Eicken, C., and Krebs, B. (2002) *Acc. Chem. Res.* **35,** 183–191
15. Cabanes, J., García-Carmona, F., García-Canovas, F., Iborra, J. L., and Lozano, J. A. (1984) *Biochim. Biophys. Acta* **790,** 101–107
16. Espin, J. C., and Wichers, H. J. (1999) *J. Agric. Food Chem.* **47,** 2638–2644
17. Hashiguchi, H., and Takahashi, H. (1977) *Mol. Pharmacol.* **13,** 362–367
18. Healey, D. F., and Strothkamp, K. G. (1981) *Arch. Biochem. Biophys.* **211,** 86–91
19. Jimenez, M., Chazarra, S., Escribano, J., Cabanes, J., and García-Carmona, F. (2001) *J. Agric. Food Chem.* **49,** 4060–4063
20. Kubo, I., and Kinst-Hori, I. (1999) *J. Agric. Food Chem.* **47,** 4121–4125
21. Maddaluno, J. F., and Faull, K. F. (1988) *Experientia (Basel)* **44,** 885–887
22. Martínez, J. H., Solano, F., Peñafiel, R., Galindo, J. D., Iborra, J. L., and Lozano, J. A. (1986) *Comp. Biochem. Physiol. B Comp. Biochem. Mol. Biol.* **83,** 633–636
23. Menon, S., Fleck, R. W., Yong, G., and Strothkamp, K. G. (1990) *Arch. Biochem. Biophys.* **280,** 27–32
24. No, J. K., Soung, D. Y., Kim, Y. J., Shim, K. H., Jun, Y. S., Rhee, S. H., Yokozawa, T., and Chung, H. Y. (1999) *Life Sci.* **65,** L241–L246
25. Bubacco, L., Vijgenboom, E., Gobin, C., Tepper, A. W. J. W., Salgado, J., and Canters, G. W. (2000) *J. Mol. Catal. B Enzymatic* **8,** 27–35
26. Tepper, A. W. J. W., Bubacco, L., and Canters, G. W. (2002) *J. Biol. Chem.* **277,** 30436–30444
27. Lippitz, M., Erker, W., Decker, H., van Holde, K. E., and Basche, T. (2002) *Proc. Natl. Acad. Sci. U. S. A.* **99,** 2772–2777
28. Schutz, J., Dolashka-Angelova, P., Abrashev, R., Nicolov, P., and Voelter, W. (2001) *Biochim. Biophys. Acta* **1546,** 325–336
29. Dolashka-Angelova, P., Hristova, R., Schuetz, J., Stoeva, S., Schwarz, H., and Voelter, W. (2000) *Spectrochim. Acta Part A Mol. Spectrosc.* **56,** 1985–1999
30. Dolashka-Angelova, P., Schick, M., Stoeva, S., and Voelter, W. (2000) *Int. J. Biochem. Cell Biol.* **32,** 529–538
31. Hristova, R., Dolashka-Angelova, P., Gigova, M., and Voelter, W. (2000) *Oxid. Commun.* **23,** 145–152
32. Pervanova, K., Idakieva, K., Stoeva, S., Genov, N., and Voelter, W. (2000)

Spectrochim. Acta Part A Mol. Spectrosc. **56,** 615–622
33. Dolashka-Angelova, P., Hristova, R., Stoeva, S., and Voelter, W. (1999) *Spectrochim. Acta Part A Mol. Spectrosc.* **55,** 2927–2934
34. Ali, S. A., Stoeva, S., Abbasi, A., Georgieva, D. N., Genov, N., and Voelter, W. (1999) *Comp. Biochem. Physiol. A* **122,** 65–74
35. Hristova, R., Dolashka, P., Stoeva, S., Voelter, W., Salvato, B., and Genov, N. (1997) *Spectrochim. Acta Part A* **53,** 471–478
36. Dolashka, P., Genov, N., Parvanova, K., Voelter, W., Geiger, M., and Stoeva, S. (1996) *Biochem. J.* **315,** 139–144
37. Idakieva, K., Stoeva, S., Voelter, W., and Genov, N. (1995) *Comp. Biochem. Physiol. B Comp. Biochem. Mol. Biol.* **112,** 599–606
38. Stoeva, S., Dolashka, P., Bankov, B., Voelter, W., Salvato, B., and Genov, N. (1995) *Spectrochim. Acta Part A Mol. Spectrosc.* **51,** 1965–1974
39. Shaklai, N., Gafni, A., and Daniel, E. (1978) *Biochemistry* **17,** 4438–4442
40. Beltramini, M., and Lerch, K. (1982) *Biochem. J.* **205,** 173–180
41. Jackman, M. P., Hajnal, A., and Lerch, K. (1991) *Biochem. J.* **274,** 707–713
42. Dean, J. A. (1999) *Lange's Handbook of Chemistry*, 15th Ed., section 5.6, McGraw-Hill, New York
43. Lerch, K., and Ettlinger, L. (1972) *Eur. J. Biochem.* **31,** 427–437
44. Fersht, A. R. (1999) *Structure and Mechanism in Protein Science: A Guide to Enzyme Catalysis and Protein Folding*, W. H. Freeman & Co., New York
45. Wilcox, D. E., Porras, A. G., Hwang, Y. T., Lerch, K., Winkler, M. E., and Solomon, E. I. (1985) *J. Am. Chem. Soc.* **107,** 4015–4027
46. Rodríguez-López, J. N., Fenoll, L. G., García-Ruiz, P. A., Varón, R., Tudela, J., Thorneley, R. N. F., and García-Cánovas, F. (2000) *Biochemistry* **39,** 10497–10506
47. Salvato, B., Santamaria, M., Beltramini, M., Alzuet, G., and Casella, L. (1998) *Biochemistry* **37,** 14065–14077
48. Eicken, C., Zippel, F., Buldt-Karentzopoulos, K., and Krebs, B. (1998) *FEBS Lett.* **436,** 293–299
49. Eicken, C., Krebs, B., and Sacchettini, J. C. (1999) *Curr. Opin. Struct. Biol.* **9,** 677–683
50. Meier, B., Scherk, C., Schmidt, M., and Parak, F. (1998) *Biochem. J.* **331,** 403–407
51. Todd, M. J., and Hausinger, R. P. (2000) *Biochemistry* **39,** 5389–5396
52. Xu, F. (1997) *J. Biol. Chem.* **272,** 924–928
53. Neri, F., Kok, D., Miller, M. A., and Smulevich, G. (1997) *Biochemistry* **36,** 8947–8953
54. Lebodia, L., Zhang, E., Lewinski, K., and Brewer, J. M. (1993) *Proteins Struct. Funct. Genet.* **16,** 219–225
55. Martinez, J. H., Solano, F., Garcia-Borron, J. C., Iborra, J. L., and Lozano, J. A. (1985) *Biochem. Int.* **11,** 729–738
56. Peñafiel, R., Galindo, J. D., Solano, F., Pedreno, E., Iborra, J. L., and Lozano, J. A. (1984) *Biochim. Biophys. Acta* **788,** 327–332
57. Belle, C., Beguin, C., Gautier-Luneau, I., Hamman, S., Philouze, C., Pierre, J. L., Thomas, F., and Torelli, S. (2002) *Inorg. Chem.* **41,** 479–491
58. Monzani, E., Quinti, L., Perotti, A., Casella, L., Gullotti, M., Randaccio, L., Geremia, S., Nardin, G., Faleschini, P., and Tabbi, G. (1998) *Inorg. Chem.* **37,** 553–562
59. Torelli, S., Belle, C., Gautier-Luneau, I., Pierre, J. L., Saint-Aman, E., Latour, J. M., Le Pape, L., and Luneau, D. (2000) *Inorg. Chem.* **39,** 3526–3536
60. Bubacco, L., van Gastel, M., Groenen, E. J., Vijgenboom, E., and Canters, G. W. (2003) *J. Biol. Chem.* **278,** 7381–7389
61. van Gastel, M., Bubacco, L., Groenen, E. J., Vijgenboom, E., and Canters, G. W. (2000) *FEBS Lett.* **474,** 228–232
62. Amudha, P., Akilan, P., and Kandaswamy, M. (1999) *Polyhedron* **18,** 1355–1362
63. Naeyaert, J. M., Eller, M., Gordon, P. R., Park, H. Y., and Gilchrest, B. A. (1991) *Br. J. Dermatol.* **125,** 297–303
64. Iwata, M., Corn, T., Iwata, S., Everett, M. A., and Fuller, B. B. (1990) *J. Investig. Dermatol.* **95,** 9–15
65. Iozumi, K., Hoganson, G. E., Pennella, R., Everett, M. A., and Fuller, B. B. (1993) *J. Investig. Dermatol.* **100,** 806–811
66. Lakowicz, J. R. (1999) *Principles of Fluorescence Spectroscopy*, 2nd Ed., pp. 242, 460, and 537, Kluwer/Plenum, Dordrecht, The Netherlands

Stopped-flow Fluorescence Studies of Inhibitor Binding to Tyrosinase from *Streptomyces antibioticus*

Armand W. J. W. Tepper, Luigi Bubacco and Gerard W. Canters

J. Biol. Chem. 2004, 279:13425-13434.
doi: 10.1074/jbc.M309367200 originally published online December 29, 2003